Culture of organoids with vestibular cell-derived factors promotes differentiation of embryonic stem cells into inner ear vestibular hair cells

Short title: *3D culture with V-CM promotes V-HC induction*

Daisuke Osaki[1, 2], Yukiteru Ouji[1]*, Masaharu Sakagami[1, 2], Tomotaka Kitamura[1], Masayasu Misu[1], Tadashi Kitahara[2], Masahide Yoshikawa[1]

[1]*Department of Pathogen, Infection and Immunity, Nara Medical University, 840 Shijo-cho, Kashihara, Nara 634-8521, Japan*

Kashihara, Nara, Japan

[2]*Department of Otolaryngology - Head and Neck Surgery, Nara Medical University, 840 Shijo-cho, Kashihara, Nara 634-8521, Japan*

***Corresponding author:**

Yukiteru Ouji

Department of Pathogen, Infection and Immunity

Nara Medical University

840 Shijo-cho, Kashihara, Nara 634-8521, Japan

Email: oujix@naramed-u.ac.jp

Email addresses of authors:

Daisuke Osaki: dosaki@naramed-u.ac.jp

Yukiteru Ouji: oujix@naramed-u.ac.jp

Masaharu Sakagami: m.sakagami@naramed-u.ac.jp

Tomotaka Kitamura: tomotaka.k@naramed-u.ac.jp

Masayasu Misu: masayasu-m@naramed-u.ac.jp

Tadashi Kitahara: tkitahara@naramed-u.ac.jp

Masahide Yoshikawa: myoshika@naramed-u.ac.jp

Vestibular hair cells (V-HCs) residing in the inner ear have important roles related to balance. Although differentiation of pluripotent stem cells into HCs has been shown, an effective method has yet to be established. We previously reported that use of vestibular cell-derived conditioned medium (V-CM) was helpful to induce embryonic stem (ES) cells to differentiate into V-HC-like cells in two-dimensional (2D) cultures of ES-derived embryoid bodies (EBs). In the present report, V-CM was used with three-dimensional (3D) cultures of EBs, which resulted in augmented expression of V-HC-related markers (Math1, Myosin6, Brn3c, Dnah5), but not of the cochlear HC-related marker Lmod3. Gene expression analyses of both 2D and 3D EBs cultured for two weeks revealed a greater level of augmented induction of HC-related markers in the 3D-cultured EBs. These results indicate that a 3D culture in combination with use of V-CM is an effective method for producing V-HCs.

Key words:

embryonic stem cells; vestibular; hair cells; organoid; differentiation; conditioned medium

Hair cells (HCs) residing in the vestibule of the inner ear have important roles related to balance (1, 2, 3). Once vestibular HCs (V-HCs) become damaged, crippling symptoms such as vertigo, visual field oscillation, and imbalance are presented (4, 5). Unfortunately, therapeutic regimens for vestibular disease are currently limited. Recently, V-HCs in mammals have been shown to have potential for turnover after cell death, albeit at a low rate (6, 7, 8, 9), with various *in vitro* and *in vivo* findings indicating spontaneous regeneration (10, 11, 12). However, the mechanism for regeneration and differentiation of V-HCs remains to be elucidated.

Pluripotent stem cells such as embryonic stem (ES) cells and induced-pluripotent stem (iPS) cells are useful sources to investigate the process of differentiation to a specific cell type. Several reports regarding their differentiation into HCs have been presented (13, 14, 15, 16). We also reported *in vitro* induction of HC-like cells from mouse ES cells using conditioned medium (CM) obtained from an ST2 stromal cell line, termed the HIST2 method (17). Those findings showing successful differentiation with use of ST2-derived CM indicated that humoral factors secreted from stromal cells have an ability to support differentiation of ES cells into HCs. Thereafter, we further demonstrated that CM from cultured vestibular cells (VCs) isolated from the inner ear supported differentiation of ES cells into vestibular HC-like cells in a cell attached condition, i.e., a two-dimensional (2D) culture (18).

For induction of various cell types or organs, including those of the inner ear, use of three-dimensional (3D) culture methods has been reported (14, 19, 20, 21). As noted above, our previous results demonstrated an important role of CM from cultured VCs (V-CM) for differentiation of V-HCs. In the present study, 3D cultures of ES-derived embryoid bodies (EBs) were performed using V-CM and that combination resulted in the augmented expression of V-HC-related markers (Math1, Myosin6, Brn3c, Dnah5).

Furthermore, gene expression analyses of 2D and 3D cultures of EBs for two weeks revealed more efficient induction of HC-related markers in 3D-cultured EBs. These results indicate that a 3D culture in combination with use of V-CM is an effective method for producing V-HCs.

MATERIALS AND METHODS

Math1-GFP ES cells

Mouse *Math1-GFP* ES cells carrying a modified GFP gene (Venus) driven by a human β-globin promoter and mouse *Math1* enhancer (22) were obtained from Dr. K. Muguruma (Kansai Medical University, Hirakata, Japan). The *Math1-GFP* ES cells were maintained in DMEM (Wako, Osaka, Japan) supplemented with 10% FBS (GIBCO, Invitrogen, Carlsbad, CA), 0.1 mM 2-mercaptoethanol (Sigma), 0.1 mM nonessential amino acids solution (GIBCO), 1 mM sodium pyruvate (Wako), and 1000 U/ml LIF (Wako) on gelatin-coated dishes without feeder cells.

Preparation and cultivation of cells derived from inner ear

C57BL/6 mice were used for this animal study under a protocol approved by Nara Medical University. Murine utricles and cochleae were isolated from inner ears of postnatal day 4 (PD4) using microdissection techniques, as previously reported (23, 24). Briefly, the utricle and cochlea covered with cartilage were exposed by fenestration of the overlying cartilaginous plate, then carefully pulled from the bone (Fig. S1A, S1B). Utricles and cochleae were separated, and cultured in ES cell medium without LIF (ES-DM), with cells proliferating around utricles and cochleae used as vestibular cells (VCs) (Fig. S1C-S1H) and cochlear cells (CCs) (Fig. S1I and S1J), respectively.

Preparation of conditioned medium (CM)

VCs and CCs were collected from the cultures of utricles and cochleae, respectively, and cultured in ES-DM. Culture supernatants of second-passaged VCs and CCs in ES-DM were collected after 24 hours, then centrifuged and filtrated through a 0.22-μm

syringe membrane filter (Merk Millipore, Billerica, MA). The filtrates were then concentrated using Amicon Ultra-15 centrifugal filter units (Merck Millipore), and finally used as VC- and CC-conditioned medium (V-CM and C-CM, respectively) (Fig. 1A).

In vitro hair cell differentiation

Undifferentiated *Math1-GFP* ES cells were dissociated using trypsin and cultured in 96-well low binding surface treated-plates (EZ-BindShut® SP, AGC Techno Glass, Japan), which resulted in formation of embryoid bodies (EBs) at a density of 3000 cells/100 μl ES-DM (25). After four days, EBs were collected and five were placed in each well of a 96-well low binding surface treated-plate (Fig. 1B), with floating 3D organoid cultures continued for a period of 15 days (Fig. 1C). As a reference, 2D cultures were also performed using attached outgrowth cultures with five EBs plated in 35-mm gelatin-coated plastic dishes for 15 days. The cultures were performed with or without 10% CM (V-CM or C-CM), with 200 μl of culture medium used for the 3D cultures and 2 ml for the 2D cultures. Half of the culture medium was changed to new medium every two days. Differentiation of *Math1-GFP* ES cells was monitored based on GFP fluorescence observed with a fluorescence microscope (BZ-X710, Keyence, Osaka, Japan).

Quantitative real-time polymerase chain reaction (qRT-PCR) analysis

Total RNA was extracted from cultured organoids using TRIzol reagent (Invitrogen), then RT-PCR were performed using a SYBR PrimeScript RT-PCR kit II (TaKaRa Bio Inc., Osaka, Japan). Primers used for PCR (TaKaRa Bio Inc.) are shown in Table S1. Relative quantitation was performed using a ΔΔCT method. Data were normalized based on the expression of *β-actin* as an endogenous control and are presented as relative gene expression.

Immunohistochemistry

Organoids were harvested, fixed with 4% PFA, and treated with 20% sucrose in PBS, then embedded in OCT compound. Sections were prepared with use of a cryostat and stained with hematoxylin-eosin (H&E). Immunofluorescence analysis was performed using a standard protocol. Briefly, organoid sections were permeabilized with 0.1% Triton X-100 in PBS containing 1% BSA (TPBS). All primary antibodies were purchased from Santa Cruz Biotechnology Inc. (Santa Cruz, CA), including anti-GFP, anti-Brn3c, anti-Myosin6, anti-a9AchR, anti-Lmod3, and anti-Dnah5, and used at the same dilution (1:100). Following incubation overnight at 4°C and washing three times with TPBS, AlexaFluor 488 or 546 conjugated anti-goat, anti-rabbit, or anti-mouse secondary antibodies (Molecular Probes, Invitrogen) were used to detect primary antibodies. All nuclei were stained with DAPI (Dojindo, Kumamoto, Japan). After incubation for one hour at room temperature and washing with TPBS three times, fluorescence was detected using fluorescence microscopy (BZ-X710).

RNA-seq

Total RNA was extracted with TRIzol reagent (Invitrogen), according to the manufacturer's protocol, while library preparation was performed based on the manufacturer's instructions using a TruSeq stranded mRNA sample prep kit (Illumina, San Diego, CA). Sequencing was performed with an Illumina HiSeq 2500 platform in 75-base single-end mode, with sequenced reads mapped to the mouse reference genome sequences (mm10) using TopHat (ver. 2.1.1) in combination with Bowtie2 (ver. 2.3.5.1) and SAMtools (ver. 1.2). The number of fragments per kilobase of exon per million mapped fragments (FPKMs) was calculated using Cufflinks (ver. 2.2.1). Access to raw data related to this study was provided under Gene Expression Omnibus (GEO) accession

number GSE214847. Data were analyzed, with heat maps, MA and scatter plots, and pathway clusters generated using the online application iDEP (ver. 0.96, http://bioinformatics.sdstate.edu/idep/).

Statistical analysis

Data are expressed as the mean ± SD of three independent experiments. Statistical significance was tested using Student's *t* test, with a p value <0.05 considered to indicate significance.

Data availability

RNA-seq raw data have been uploaded to Gene Expression Omnibus (GEO) with accession number GSE214847.

RESULTS

Morphology and GFP-positivity of *Math1-GFP* ES cells in 3D cultures

EBs cultured for four days in 96-well plates were subjected to culturing with ES-DM or V-CM for 15 days (Fig. 2). Organoids cultured with V-CM formed distinct cysts surrounding EB-derived spheres (Fig. 2B, 2D, 2F; Fig. S2, V-CM). On the other hand, no apparent cysts were formed in organoids cultured with ES-DM (Fig. 2A, 2C, 2E; Fig. S2, ES-DM). In observations of *Math1*-derived GFP fluorescence, GFP-positive cells were detected in organoids cultured with V-CM (Fig. 2B, 2D, 2F; Fig. S2, V-CM), but not in those cultured with ES-DM (Fig. 2A, 2C, 2E; Fig. S2, ES-DM). These results indicated that V-CM effectively induced differentiation of the present ES cells into *Math1*-positive cells.

Gene expression analysis of hair cell (HC)-related markers

Total RNA was extracted from organoids cultured with ES-DM or V-CM for 15 days, then gene expressions of HC-related markers were examined using a real-time qRT-PCR method. The HC-related markers *Math1*, *Myosin6*, and *Brn3c* were significantly increased in organoids cultured with V-CM as compared to those cultured with ES-DM (Fig. 3A). As for differential development between cochlear and vestibular HCs, *Lmod3* and *Dnah5*, respectively, have been reported as potential markers (26). Therefore, we examined the expressions of *Lmod3* and *Dnah5*, and found increased expression of *Dnah5,* the marker used for V-HCs, in organoids cultured with V-CM as compared to ES-DM, whereas there was no significant difference regarding gene expression of *Lmod3* in organoids cultured with either of the medium formulations (Fig. 3B), suggesting an ability of V-CM to induce V-HC. Although our previous study demonstrated that V-CM

supported differentiation of ES cells into V-HC-like cells in 2D cultures (18), expressions of *Math1, Myosin6, Brn3c*, and *Dnah5* were more efficiently induced in the present 3D culture setting (Fig. S3).

Immunocytochemical analysis of hair cell-related markers

Section analysis of organoids cultured for 15 days with ES-DM or V-CM was performed (Fig. 4). Using H&E staining, cyst-like structures were found in sections of organoids cultured with V-CM, but not in those cultured with ES-DM (Fig. 4A, 4B). Next, an immunocytochemical examination of expressions of HC-related markers in organoids cultured with ES-DM or V-CM for 15 days was performed. In organoids cultured with ES-DM, no *Math1*-derived GFP expression nor that of any of the HC-related markers, including Brn3c, Myosin6, a9AchR, Lmod3, and Dnah5, was observed (Fig 4C, 4E, 4G, 4I, 4K; Fig. S4, ES-DM). On the other hand, *Math1*-derived GFP-positive cells were clearly observed in organoids cultured with V-CM and those showed simultaneous expression of Brn3c, Myosin6, a9AchR, and Dnah5 (Fig. 4D, 4F, 4H, 4L; Fig. S4, V-CM). Interestingly, Lmod3-immunopositive cells were not detected in organoids cultured with V-CM (Fig. 4J; Fig. S4, V-CM). These results revealed that differentiation of ES cells into vestibular HC-like cells was promoted in organoids cultured with V-CM.

Gene expression analysis of ES cell-derived organoids cultured in conditioned medium (CM)

The present study was performed as an attempt to specifically induce differentiation of ES cells into V-HCs using V-CM. Since the inner ear contains C-HCs (27), CC-derived conditioned medium (C-CM) was prepared. However, in contrast to V-CM, it was found that C-CM had no enhancing effect on the expression of *Dnah5*, a V-HC marker (Fig. 5),

indicating that V-CM contains specific factors associated with V-HC induction.

Next, to broadly explore candidate factors for V-HC induction in V-CM, an RNA-seq method was employed to compare gene expressions between VCs and CCs (Fig. 6A). The expression levels of 502 genes were found to be significantly increased in the VCs as compared to the CCs, while those of 659 genes were decreased (Fig. 6B-6D). Such differentially expressed genes (DEGs) were primarily observed in pathways related to extracellular matrix organization, system development, tissue development, and other such activities (Fig. 6E, Table S2). Notably, some extracellular matrices (ECMs) including collagen matrix genes, such as *Col14a1, Col2a1, Col5a2, Col3a1, Col11a1, Col15a1, Col1a2, Col8a2*, and *Col8a1*, were found to be upregulated in VCs (Table S3).

DISCUSSION

Although methods for induction of hair cell (HC) differentiation using gene transfer, addition of various cytokines, and use of feeder cells have been reported (28, 29, 30, 31), the techniques are complicated. In on our previous study, successful induction of differentiation from mouse ES cells into HC-like cells using CM from ST2 cells of a mouse bone marrow-derived stromal cell line with a simple procedure, termed the HIST2 method (17), was noted. Therefore, cell-derived CM was thought usable for simplifying induction of HC differentiation.

HCs are present in the cochlea and vestibule of the inner ear, and undergo a distinct differentiation process (27, 32, 33). However, there have been very few *in vitro* studies that examined regulation of vestibular and cochlear HC differentiation (34). In our previous investigation, vestibular cells (VCs) isolated from the inner ear of mice showed selective induction of differentiation from mouse ES cells into vestibular HCs (V-HCs) with use of V-CM (18). In the present study, we attempted to develop a more efficient method of differentiation induction using V-CM.

Recently, 3D culture methods have been used for induction of cells related to various organs, including intestines (35), brain (36), liver (37), and inner ear (14). A recent report regarding neuronal differentiation from iPS also showed that 3D were more efficient than 2D cultures (38). Among the various factors that influence differentiation, such as spontaneous self-organizing ability, cell polarity, membrane contacts, and morphogen gradients, a key difference between 2D and 3D cultures is differential contact between cells and the ECM, which is known to affect a variety of cellular behaviors, including differentiation, cell growth, and motility (39, 40). Indeed, gene expression analysis of *Oct-3/4*, an undifferentiated marker of ES cells, revealed a subtle level of expression in

2D cultures after 15 days, where none was noted in 3D cultures (Fig. S5).

A large number of cysts were formed in the 3D cultures with V-CM (Fig. 2B, 2D, 2F; Fig. S2, V-CM). Koehler *et al.* reported induction of cyst formation in organoids with use of their method, with HCs mainly detected along cyst edges (14). In the present study, while organoid sections showed distinct cyst formation (Fig. 4B), expressions of HC-related markers were detected inside cysts with use of an immunohistochemical method (Fig. 4D, 4F, 4H, 4L; Fig. S3, V-CM). These differing results may be related to the different culture procedures, as the study by Koehler *et al.* used single EBs, principally expanding outward, while the present study used five EBs, with aggregation initiated from contacted surfaces and/or the presence of unknown cytokines in V-CM. In addition, the expression level of *Math1*-derived GFP was lower on Day 15 as compared to Day 5 and 10 (Fig. 2, S2). *Math1* is known to be expressed in pro-sensory epithelium and HCs, but not in supporting cells (SCs) during development of the inner ear (41, 42). Therefore, a decrease in GFP fluorescence may reflect an increase in SC-like cells.

Although previous studies have reported induction of HC differentiation (14, 15, 16), the only specific method available to induce V-HC differentiation is use of V-CM, as noted in our previous report (18) as well as in the present findings. To explore induction factors in V-CM that promote differentiation of ES cells into V-HCs, RNA-seq gene expression analysis was performed using VCs and CCs, which showed a higher level of expression of ECMs in VCs as compared to CCs (Fig. 6, Table S2, S3). Genes related to the biosynthesis of the ECM, such as collagen (43) and lysyl oxidase (44) family genes, and *Serpinh1* (also known as *Hsp47*) (45, 46), were found to be enriched in DEGs. An explanation for why V-CM favorably induces differentiation of V-HCs may due to ECM composition, though it will be necessary to perform examinations using recombinant proteins to determine factors related to V-HC induction. Additionally, culture method

improvements, such as a different of V-CM and/or adjusting the timing of its addition, may result in more efficient induction of V-HCs.

ACKNOWLEDGMENTS

This work was supported by a Grant-in-Aid for Scientific Research (B) (to Y.O. and M.Y.) (16H05482) from the Ministry of Education, Culture, Sports, Science and Technology of Japan (KAKENHI). We thank Dr. K. Muguruma (Kansai Medical University, Hirakata, Japan) for the *Math1-GFP* ES cell lines, Dr. Okuzaki (Genome Information Research Center, Research Institute for Microbial Diseases, Osaka University, Suita, Japan) for performing the RNA-seq analysis, and S. Shimada for technical assistance. DO, YO, MS, and MM performed the experiments and statistical analysis. YO and MY conceived and designed the experiments. TK and TK contributed to preparation of the manuscript. DO, YO, and MY wrote the manuscript. All authors have read and approved the final version of the manuscript. The authors have no competing interests to declare.

References

1. **Wiest, G.:** The origins of vestibular science, Annals of the New York Academy of Sciences, **1343**, 1-9 (2015).
2. **Day, B. L. and Fitzpatrick, R. C.:** The vestibular system, Current biology : CB, **15**, R583-586 (2005).
3. **Baloh, R. W. and Honrubia, V.:** The central vestibular system, Contemp Neurol Ser, **18**, 47-99 (1979).
4. **Klingner, C. M., Axer, H., Brodoehl, S., and Witte, O. W.:** Vertigo and the processing of vestibular information: A review in the context of predictive coding, Neurosci Biobehav Rev, **71**, 379-387 (2016).
5. **Iwasaki, S. and Yamasoba, T.:** Dizziness and Imbalance in the Elderly: Age-related Decline in the Vestibular System, Aging Dis, **6**, 38-47 (2015).
6. **Burns, J. C. and Stone, J. S.:** Development and regeneration of vestibular hair cells in mammals, Seminars in cell & developmental biology, **65**, 96-105 (2017).
7. **Li, W., You, D., Chen, Y., Chai, R., and Li, H.:** Regeneration of hair cells in the mammalian vestibular system, Frontiers of medicine, **10**, 143-151 (2016).
8. **Wang, T., Chai, R., Kim, G. S., Pham, N., Jansson, L., Nguyen, D. H., Kuo, B., May, L. A., Zuo, J., Cunningham, L. L., and Cheng, A. G.:** Lgr5+ cells regenerate hair cells via proliferation and direct transdifferentiation in damaged neonatal mouse utricle, Nature communications, **6**, 6613 (2015).
9. **Rubel, E. W., Dew, L. A., and Roberson, D. W.:** Mammalian vestibular hair cell regeneration., Science, **267**, 701-707 (1995).
10. **Taylor, R. R., Filia, A., Paredes, U., Asai, Y., Holt, J. R., Lovett, M., and Forge, A.:** Regenerating hair cells in vestibular sensory epithelia from humans,

eLife, 7 (2018).

11. **Staecker, H., Praetorius, M., Baker, K., and Brough, D. E.:** Vestibular hair cell regeneration and restoration of balance function induced by math1 gene transfer., Otology & neurotology : official publication of the American Otological Society, American Neurotology Society [and] European Academy of Otology and Neurotology, **28**, 223-231 (2007).

12. **Huang, Y. B., Ma, R., Yang, J. M., Han, Z., Cong, N., Gao, Z., Ren, D., Wang, J., and Chi, F. L.:** Cell proliferation during hair cell regeneration induced by Math1 in vestibular epithelia in vitro, Neural regeneration research, **13**, 497-501 (2018).

13. **Ouji, Y., Ishizaka, S., Nakamura-Uchiyama, F., Wanaka, A., and Yoshikawa, M.:** Induction of inner ear hair cell-like cells from Math1-transfected mouse ES cells, Cell death & disease, **4**, e700 (2013).

14. **Koehler, K. R., Mikosz, A. M., Molosh, A. I., Patel, D., and Hashino, E.:** Generation of inner ear sensory epithelia from pluripotent stem cells in 3D culture, Nature, **500**, 217-221 (2013).

15. **Oshima, K., Shin, K., Diensthuber, M., Peng, A. W., Ricci, A. J., and Heller, S.:** Mechanosensitive hair cell-like cells from embryonic and induced pluripotent stem cells, Cell, **141**, 704-716 (2010).

16. **Koehler, K. R., Nie, J., Longworth-Mills, E., Liu, X. P., Lee, J., Holt, J. R., and Hashino, E.:** Generation of inner ear organoids containing functional hair cells from human pluripotent stem cells, Nat Biotechnol, **35**, 583-589 (2017).

17. **Ouji, Y., Ishizaka, S., Nakamura-Uchiyama, F., and Yoshikawa, M.:** In vitro differentiation of mouse embryonic stem cells into inner ear hair cell-like cells using stromal cell conditioned medium, Cell death & disease, **3**, e314 (2012).

18. **Sakagami, M., Ouji, Y., Kawai, N., Misu, M., Yoshikawa, M., and Kitahara, T.:** Differentiation of embryonic stem cells into inner ear vestibular hair cells using vestibular cell derived-conditioned medium, Biochem Biophys Rep, **19**, 100649 (2019).

19. **Ueda, K., Onishi, A., Ito, S. I., Nakamura, M., and Takahashi, M.:** Generation of three-dimensional retinal organoids expressing rhodopsin and S- and M-cone opsins from mouse stem cells, Biochemical and biophysical research communications, **495**, 2595-2601 (2018).

20. **Dye, B. R., Hill, D. R., Ferguson, M. A., Tsai, Y. H., Nagy, M. S., Dyal, R., Wells, J. M., Mayhew, C. N., Nattiv, R., Klein, O. D., and other XXX authors:** In vitro generation of human pluripotent stem cell derived lung organoids, eLife, **4** (2015).

21. **Volkner, M., Zschatzsch, M., Rostovskaya, M., Overall, R. W., Busskamp, V., Anastassiadis, K., and Karl, M. O.:** Retinal Organoids from Pluripotent Stem Cells Efficiently Recapitulate Retinogenesis, Stem cell reports, **6**, 525-538 (2016).

22. **Su, H. L., Muguruma, K., Matsuo-Takasaki, M., Kengaku, M., Watanabe, K., and Sasai, Y.:** Generation of cerebellar neuron precursors from embryonic stem cells, Developmental biology, **290**, 287-296 (2006).

23. **Brandon, C. S., Voelkel-Johnson, C., May, L. A., and Cunningham, L. L.:** Dissection of adult mouse utricle and adenovirus-mediated supporting-cell infection, Journal of visualized experiments : JoVE, **61**, 3734 (2012).

24. **Oshima, K., Senn, P., and Heller, S.:** Isolation of sphere-forming stem cells from the mouse inner ear, Methods in molecular biology, **493**, 141-162 (2009).

25. **Keller, G. M.:** In vitro differentiation of embryonic stem cells, Current opinion

in cell biology, **7**, 862-869 (1995).

26. **Scheffer, D. I., Shen, J., Corey, D. P., and Chen, Z. Y.:** Gene Expression by Mouse Inner Ear Hair Cells during Development, The Journal of neuroscience : the official journal of the Society for Neuroscience, **35**, 6366-6380 (2015).

27. **Raft, S. and Groves, A. K.:** Segregating neural and mechanosensory fates in the developing ear: patterning, signaling, and transcriptional control, Cell and tissue research, **359**, 315-332 (2015).

28. **Lee, S., Song, J. J., Beyer, L. A., Swiderski, D. L., Prieskorn, D. M., Acar, M., Jen, H. I., Groves, A. K., and Raphael, Y.:** Combinatorial Atoh1 and Gfi1 induction enhances hair cell regeneration in the adult cochlea, Scientific reports, **10**, 21397 (2020).

29. **Lahlou, H., Lopez-Juarez, A., Fontbonne, A., Nivet, E., and Zine, A.:** Modeling human early otic sensory cell development with induced pluripotent stem cells, PloS one, **13**, e0198954 (2018).

30. **Ding, J., Tang, Z., Chen, J., Shi, H., Chen, J., Wang, C., Zhang, C., Li, L., Chen, P., and Wang, J.:** Induction of differentiation of human embryonic stem cells into functional hair-cell-like cells in the absence of stromal cells, The international journal of biochemistry & cell biology, **81**, 208-222 (2016).

31. **Saeki, T., Yoshimatsu, S., Ishikawa, M., Hon, C. C., Koya, I., Shibata, S., Hosoya, M., Saegusa, C., Ogawa, K., Shin, J. W., Fujioka, M., and Okano, H.:** Critical roles of FGF, RA, and WNT signalling in the development of the human otic placode and subsequent lineages in a dish, Regen Ther, **20**, 165-186 (2022).

32. **McLean, W. J., McLean, D. T., Eatock, R. A., and Edge, A. S.:** Distinct capacity for differentiation to inner ear cell types by progenitor cells of the

cochlea and vestibular organs, Development, **143**, 4381-4393 (2016).

33. **Atkinson, P. J., Huarcaya Najarro, E., Sayyid, Z. N., and Cheng, A. G.:** Sensory hair cell development and regeneration: similarities and differences, Development, **142**, 1561-1571 (2015).

34. **Zhang, Y., Tang, Q., Xue, R., Gao, J., Yang, H., Gao, Z., and Lin, G.:** Absence of Atoh1 induced partially different cell fates of cochlear and vestibular sensory epithelial cells in mice, Acta oto-laryngologica, **138**, 972-976 (2018).

35. **Yoshida, S., Miwa, H., Kawachi, T., Kume, S., and Takahashi, K.:** Generation of intestinal organoids derived from human pluripotent stem cells for drug testing, Scientific reports, **10**, 5989 (2020).

36. **Sgodda, M., Dai, Z., Zweigerdt, R., Sharma, A. D., Ott, M., and Cantz, T.:** A Scalable Approach for the Generation of Human Pluripotent Stem Cell-Derived Hepatic Organoids with Sensitive Hepatotoxicity Features, Stem cells and development, **26**, 1490-1504 (2017).

37. **Muguruma, K.:** Self-Organized Cerebellar Tissue from Human Pluripotent Stem Cells and Disease Modeling with Patient-Derived iPSCs, Cerebellum, **17**, 37-41 (2018).

38. **Scuderi, S., Altobelli, G. G., Cimini, V., Coppola, G., and Vaccarino, F. M.:** Cell-to-Cell Adhesion and Neurogenesis in Human Cortical Development: A Study Comparing 2D Monolayers with 3D Organoid Cultures, Stem cell reports, **16**, 264-280 (2021).

39. **Engler, A. J., Sen, S., Sweeney, H. L., and Discher, D. E.:** Matrix elasticity directs stem cell lineage specification, Cell, **126**, 677-689 (2006).

40. **Saha, K., Keung, A. J., Irwin, E. F., Li, Y., Little, L., Schaffer, D. V., and Healy, K. E.:** Substrate modulus directs neural stem cell behavior, Biophysical

journal, **95**, 4426-4438 (2008).

41. **Woods, C., Montcouquiol, M., and Kelley, M. W.:** Math1 regulates development of the sensory epithelium in the mammalian cochlea, Nature neuroscience, **7**, 1310-1318 (2004).

42. **Cotanche, D. A. and Kaiser, C. L.:** Hair cell fate decisions in cochlear development and regeneration, Hearing research, **266**, 18-25 (2010).

43. **Wu, H., Che, S., Li, S., Cheng, Y., Xiao, J., and Liu, Z.:** Case report of the first molecular diagnosis of Stickler syndrome with a pathogenic COL2A1 variant in a Mongolia family, Mol Genet Genomic Med, **9**, e1781 (2021).

44. **Liu, Z., Bai, X., Wan, P., Mo, F., Chen, G., Zhang, J., and Gao, J.:** Targeted Deletion of Loxl3 by Col2a1-Cre Leads to Progressive Hearing Loss, Front Cell Dev Biol, **9**, 683495 (2021).

45. **Nagai, N., Hosokawa, M., Itohara, S., Adachi, E., Matsushita, T., Hosokawa, N., and Nagata, K.:** Embryonic lethality of molecular chaperone hsp47 knockout mice is associated with defects in collagen biosynthesis, The Journal of cell biology, **150**, 1499-1506 (2000).

46. **De Silva, M. G., Hildebrand, M. S., Christopoulos, H., Newman, M. R., Bell, K., Ritchie, M., Smyth, G. K., and Dahl, H. H.:** Gene expression changes during step-wise differentiation of embryonic stem cells along the inner ear hair cell pathway, Acta oto-laryngologica, **126**, 1148-1157 (2006).

Figure legends

Fig. 1. Preparation of vestibular cell (VC)-derived conditioned medium and *in vitro* differentiation procedure using 3D culture method. (A) Conditioned medium (CM) was collected from 24-hour cultures of second-passaged VCs. After centrifugation and filtration of the CM, the filtrate was concentrated using centrifugal filter units and then used as VC-conditioned medium (V-CM). (B) Images obtained at start of 3D culture of five EBs. Scale bar = 100 μm. (C) Procedure for *in vitro* HC differentiation using 3D culture.

Fig. 2. Observations of *Math1-GFP* ES cell-derived organoids cultured with ES-DM or V-CM. (A, C, E) Morphology and GFP expression of *Math1-GFP* ES cell-derived organoids cultured with ES-DM on days 5, 10, and 15. (B, D, F) Morphology and GFP expression of *Math1-GFP* ES cell-derived organoids cultured with V-CM on days 5, 10, and 15. Scale bar = 100 μm.

Fig. 3. Gene expression analysis of HC-related markers in *Math1-GFP* ES cell-derived organoids cultured with ES-DM or V-CM. Gene expressions of hair cell (HC)-related markers were examined using a real-time qRT-PCR method. (A) Gene expressions of HC markers *Math1*, *Myosin6*, and *Brn3c*. (B) Gene expressions of *Lmod3* and *Dnah5* (cochlear and vestibular HC-related marker, respectively). Values were normalized to that of *β-actin* expression, used as an endogenous control. N=3, $^*p$ <0.05, n.s.; not significant.

Fig. 4. Immunocytochemical analysis of HC-related markers expressed in *Math1-GFP* ES cell-derived organoids cultured with ES-DM or V-CM. (A, B) Sections of *Math1-GFP* ES cell-derived organoids cultured with ES-DM (A) or V-CM (B), then subjected to H&E staining. Scale bar = 500 μm. (C-L) Expressions of HC-related markers in *Math1-GFP* ES cell-derived organoids cultured with ES-DM or V-CM for two weeks were examined using an immunocytochemical method. Neither HC-related markers nor *Math1*-derived GFP were detected in organoids cultured with ES-DM (C, E, G, I, K), whereas most of the *Math1*-derived GFP positive cells in organoids cultured with V-CM showed simultaneous expression of Brn3c (D), Myosin6 (F), a9AchR (H), and Dnah5 (L). On the other hand, no Lmod3-immunopositive cells were detected in organoids cultured with V-CM, whereas *Math1*-derived GFP positive cells were observed (J). Scale bar = 200 μm.

Fig. 5. Gene expression analysis of V-HC marker *Dnah5* in *Math1-GFP* ES cell-derived organoids cultured with ES-DM, V-CM, or C-CM. The gene expression of *Dnah5* by *Math1-GFP* ES cells cultured in ES-DM, V-CM, or C-CM for two weeks was examined using real-time RT-PCR. Data were normalized to *β-actin* expression, used as an endogenous control. N=3, $*p < 0.05$.

Fig. 6. RNA-seq analysis for VC and CC. (A) Heat map for visualization of raw count data obtained with online application iDEP (ver. 0.96, http://bioinformatics.sdstate.edu/idep/). (B) Identified differential expressed genes (DEGs) were extracted using DESEq2. There were 502 upregulated and 659 downregulated genes. (C, D) Colored dots show significantly upregulated (red) and downregulated (blue) genes in MA (C) and scatter (D) plots. (E) Cluster of pathways

enriched in DEGs.

Fig. 1.

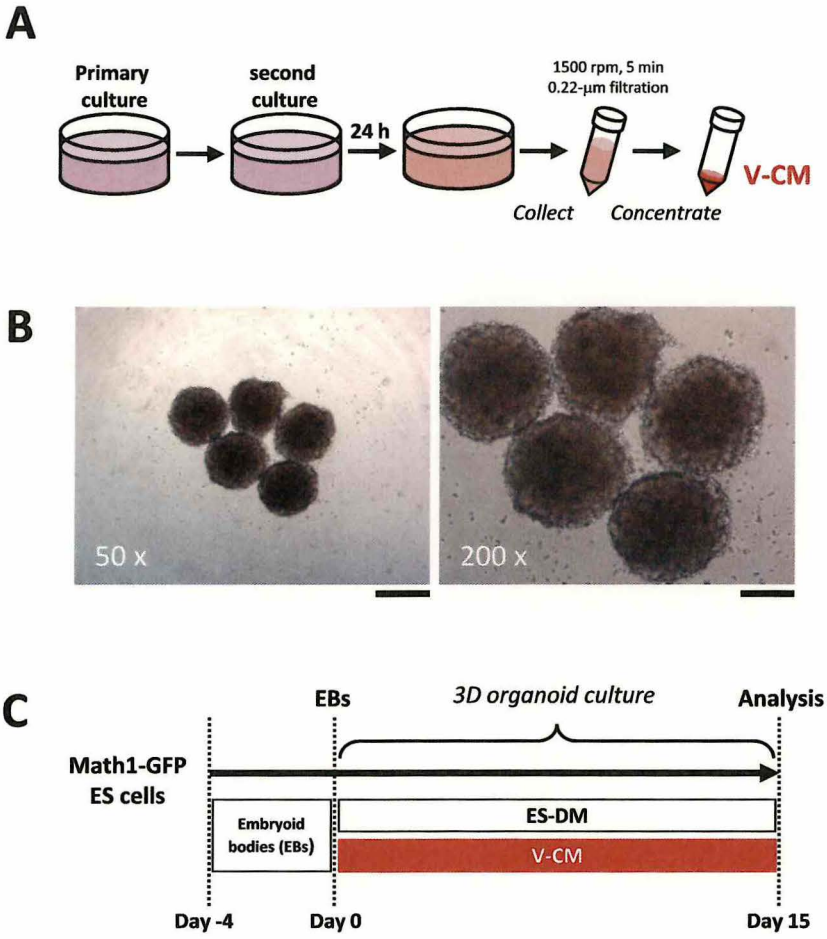
A
Primary culture
second culture
24 h
1500 rpm, 5 min
0.22-μm filtration
V-CM
Collect
Concentrate
B
50 x
200 x
C
EBs
3D organoid culture
Analysis
Math1-GFP ES cells
Embryoid bodies (EBs)
ES-DM
V-CM
Day -4
Day 0
Day 15

Fig. 2.

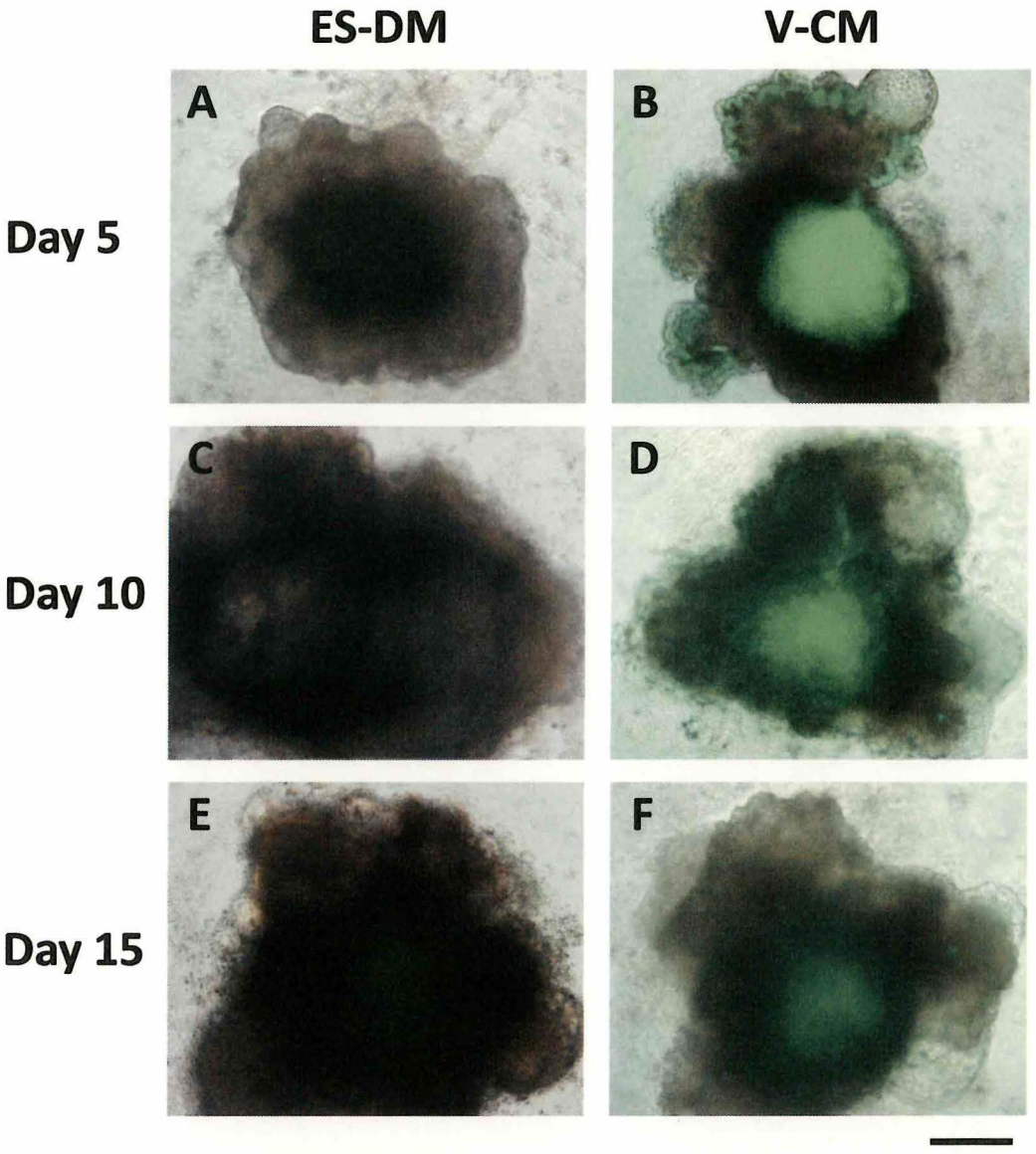

Fig. 3.

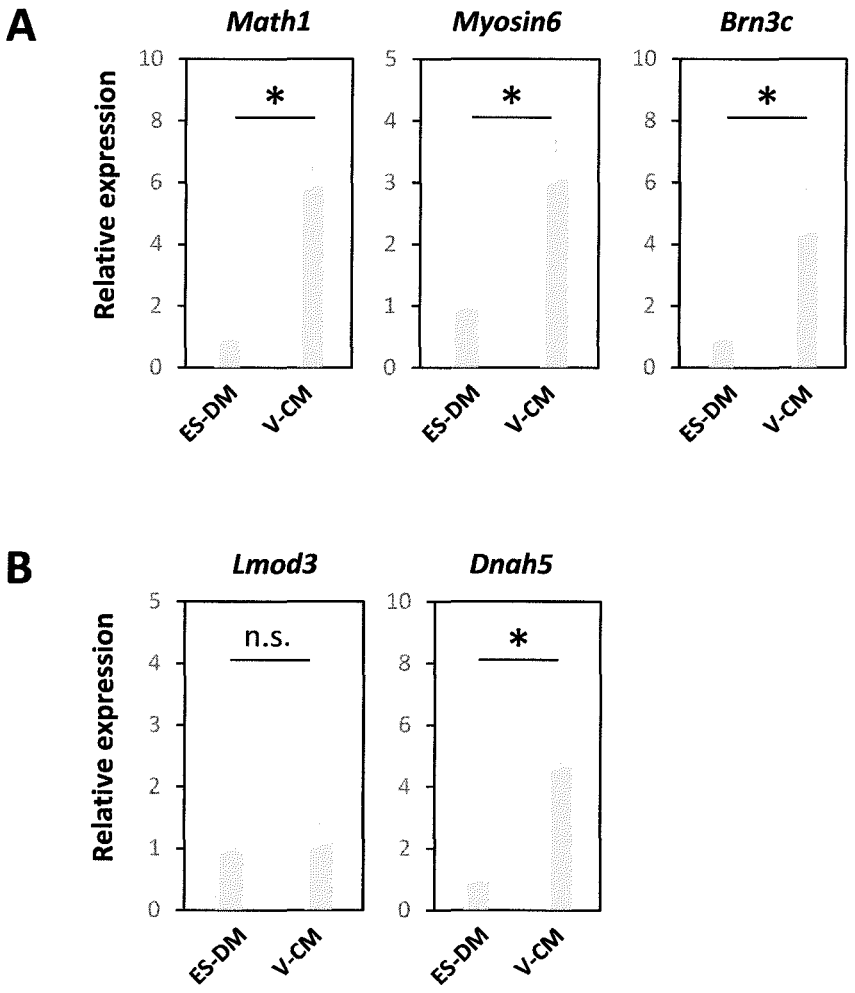
A
Math1
Myosin6
Brn3c
Relative expression
10
8
6
4
2
0
5
4
3
2
1
0
*
ES-DM
V-CM
B
Lmod3
Dnah5
n.s.

Fig. 4.

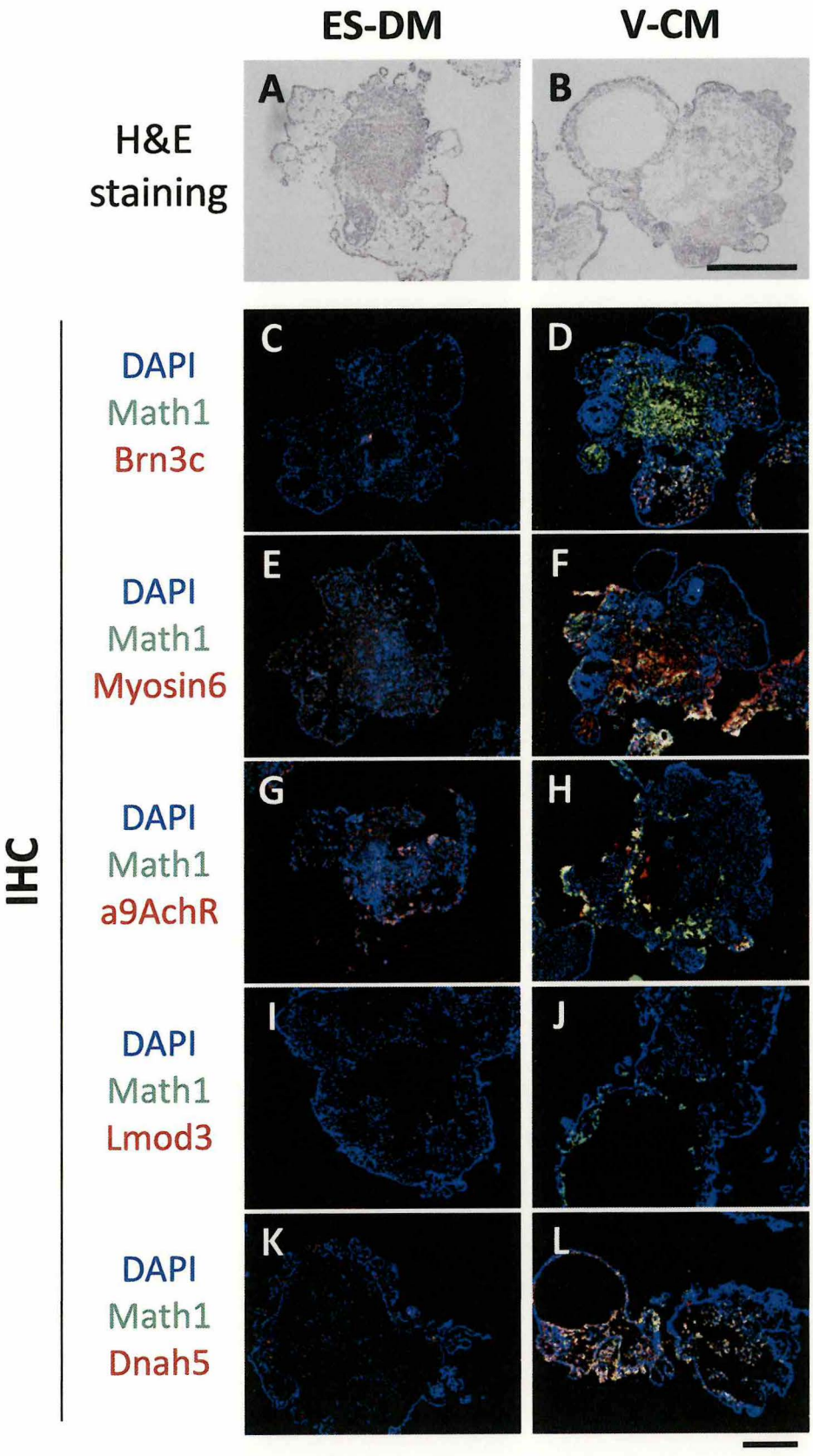
ES-DM
V-CM
H&E staining
A
B
IHC
DAPI
Math1
Brn3c
C
D
DAPI
Math1
Myosin6
E
F
DAPI
Math1
a9AchR
G
H
DAPI
Math1
Lmod3
I
J
DAPI
Math1
Dnah5
K
L

Fig. 5.

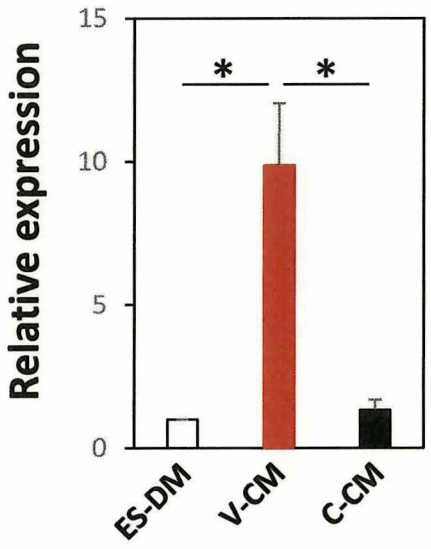

Fig. 6.

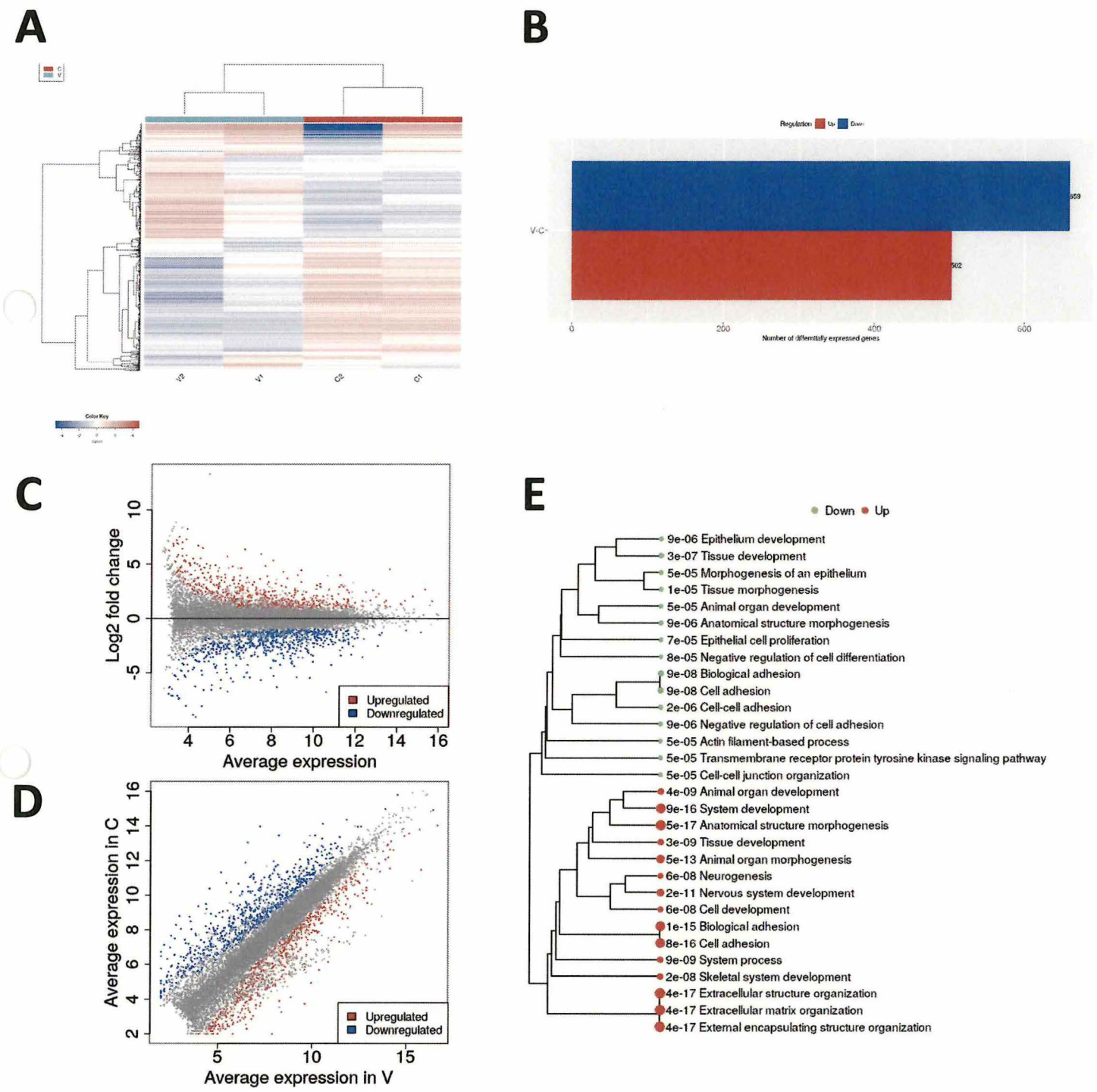
A
B
C
D
E
Log2 fold change
Average expression
Upregulated
Downregulated
Average expression in C
Average expression in V
Down
Up
9e-06 Epithelium development
3e-07 Tissue development
5e-05 Morphogenesis of an epithelium
1e-05 Tissue morphogenesis
5e-05 Animal organ development
9e-06 Anatomical structure morphogenesis
7e-05 Epithelial cell proliferation
8e-05 Negative regulation of cell differentiation
9e-08 Biological adhesion
9e-08 Cell adhesion
2e-06 Cell-cell adhesion
9e-06 Negative regulation of cell adhesion
5e-05 Actin filament-based process
5e-05 Transmembrane receptor protein tyrosine kinase signaling pathway
5e-05 Cell-cell junction organization
4e-09 Animal organ development
9e-16 System development
5e-17 Anatomical structure morphogenesis
3e-09 Tissue development
5e-13 Animal organ morphogenesis
6e-08 Neurogenesis
2e-11 Nervous system development
6e-08 Cell development
1e-15 Biological adhesion
8e-16 Cell adhesion
9e-09 System process
2e-08 Skeletal system development
4e-17 Extracellular structure organization
4e-17 Extracellular matrix organization
4e-17 External encapsulating structure organization

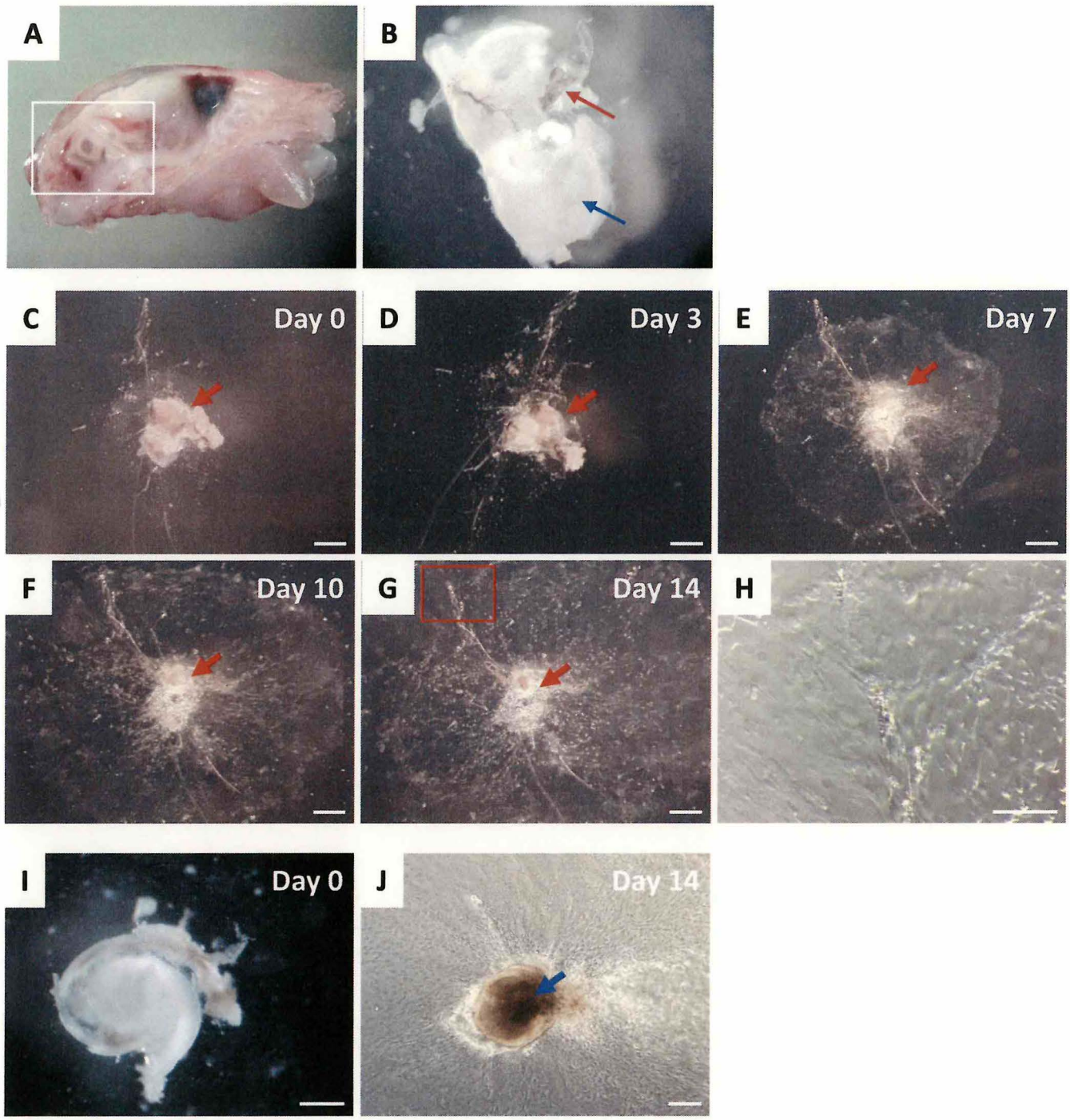

Fig. S1. Preparation and morphology of vestibular cells (VCs) and cochlear cells (CCs) isolated from mouse inner ear.

(A) Head of postnatal day 4 (PD4) C57BL/6 mouse.

(B) Inner ear tissue, indicated by a white square in A, was isolated using a microdissection method. Red and blue arrows indicate utricle and cochlea, respectively.

(C-G) Isolated utricles (red arrows) were cultured with ES-DM for two weeks. Photographs show outgrowths on day 0 (C), day 3 (D), day 7 (E) day 10 (F), and day 14 (G). Scale bar = 500 μm

(H) High magnification view of red square areas in (G). Scale bar = 100 μm

(I,J) Images show isolated cochlea (I) and outgrowths cultured with ES-DM for two weeks (J). Scale bar = 500 μm

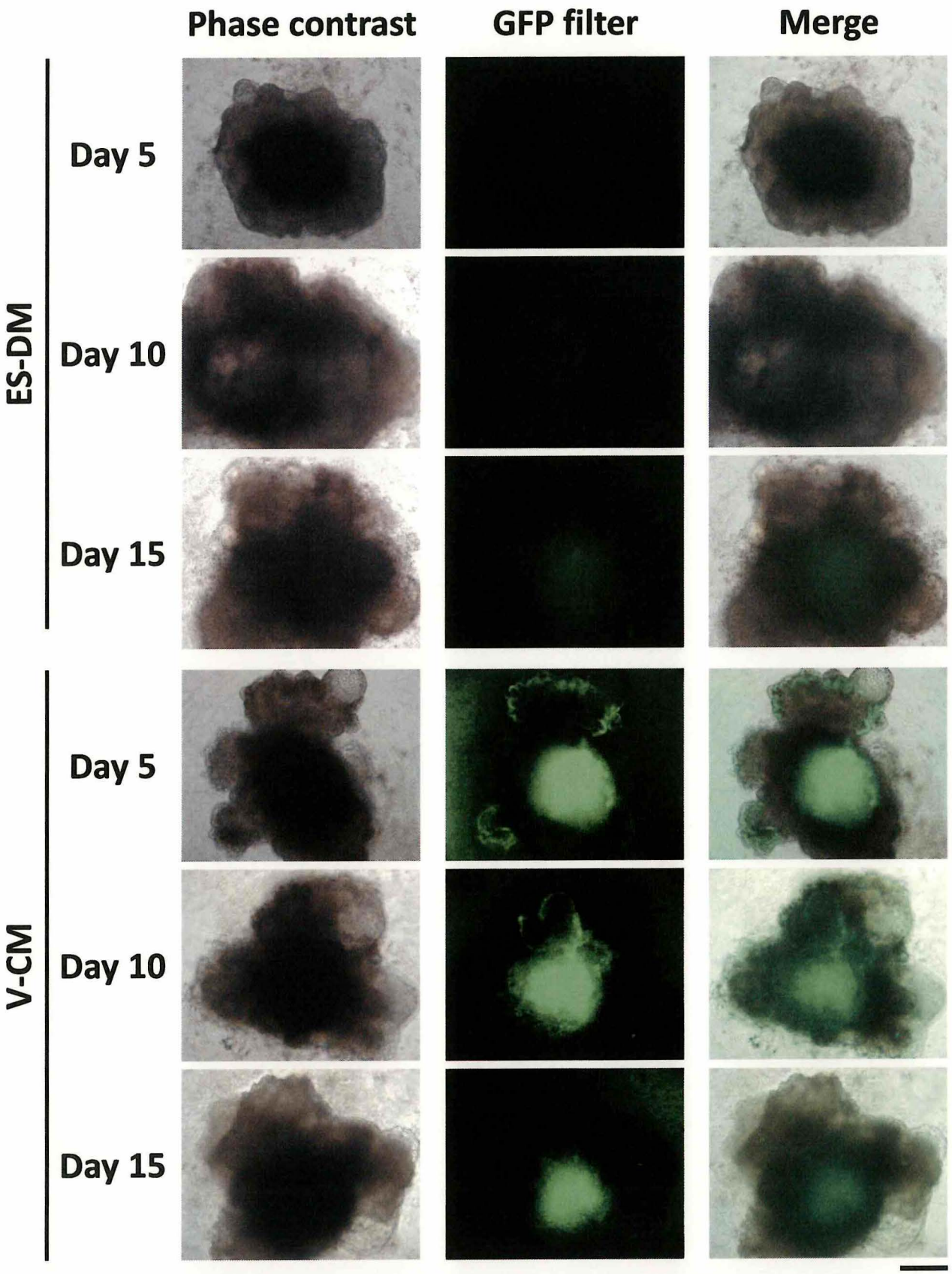

Fig. S2. *Math1*-GFP ES cell-derived organoids cultured with ES-DM or V-CM.
(ES-DM) Morphology and GFP expression of *Math1*-GFP ES cell-derived organoids cultured with ES-DM on day 5, day 10, and day 15.
(V-CM) Morphology and GFP expression of *Math1*-GFP ES cell-derived organoids cultured with V-CM on day 5, day 10, and day 15. Scale bar = 100 μm

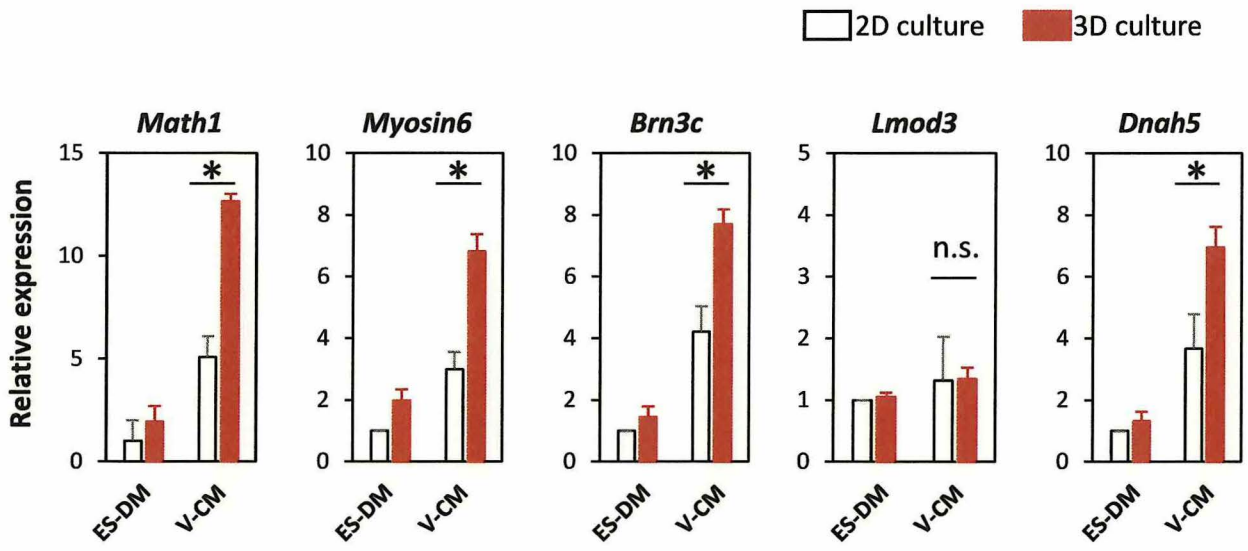

Fig. S3. Gene expression analysis of HC-related markers in *Math1-GFP* ES cell-derived organoids cultured with ES-DM or V-CM using 2D or 3D cultures.

Gene expressions of *Math1*, *Myosin6*, and *Brn3c*, (HC-related markers), *Lmod3* (cochlear HC-related marker), and *Dnah5* (vestibular HC-related marker) in *Math1-GFP* ES cell-derived organoids cultured with ES-DM or V-CM using 2D (white bars) or 3D cultures (red bars) for two weeks were examined by real-time RT-PCR. Values were normalized to that of *β-actin* expression, used as an endogenous control. N=3, *p <0.05, n.s.; not significant

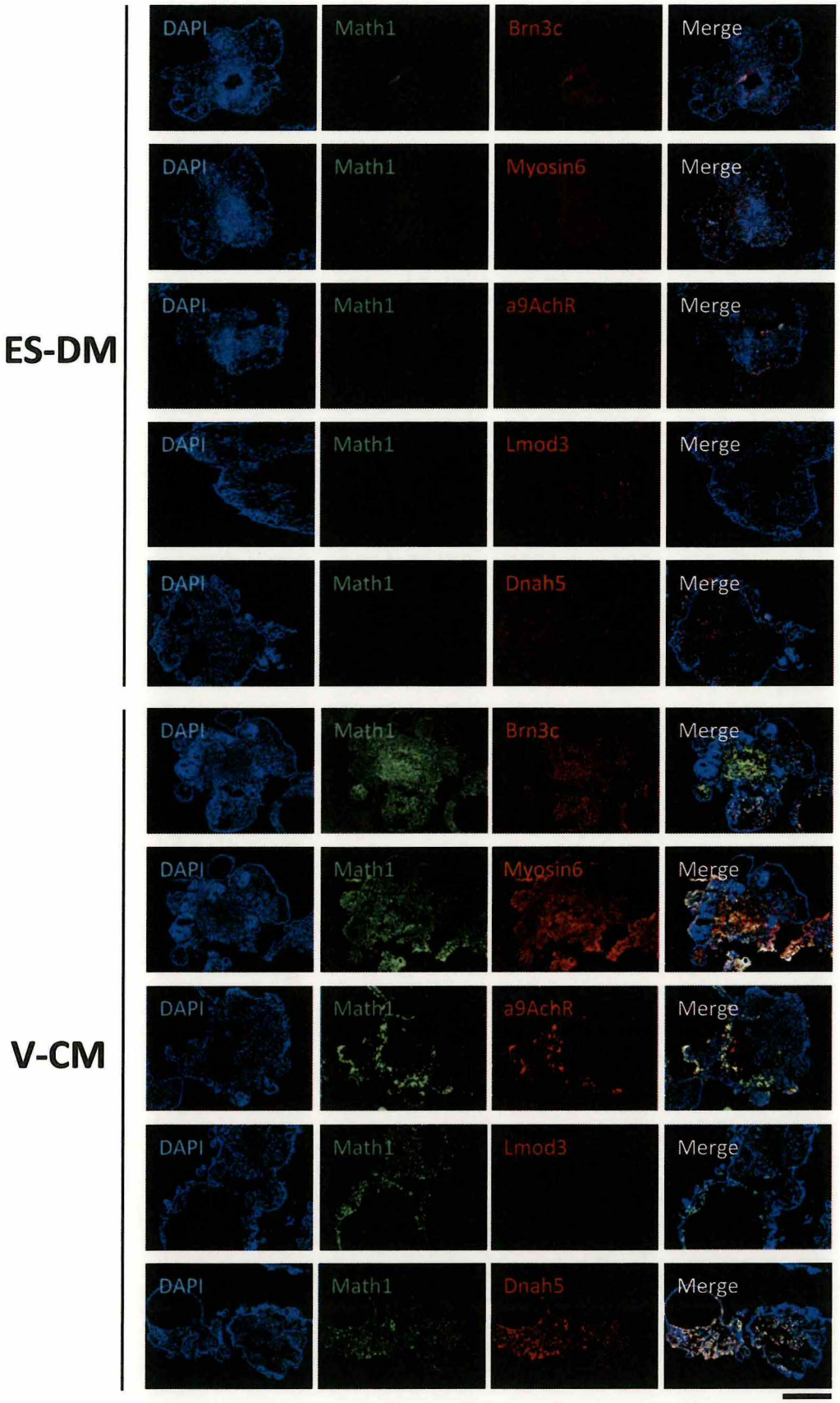

Fig. S4. Immunocytochemical analysis of HC-related markers expressed in *Math1-GFP* ES cell-derived organoids cultured with ES-DM or V-CM.
(ES-DM) Neither HC-related markers nor *Math1*-derived GFP were detected in organoids cultured with ES-DM (V-CM). Most of *Math1*-derived GFP-positive cells found in organoids cultured with V-CM simultaneously expressed Brn3c, Myosin6, a9AchR, and Dnah5, but not Lmod3. Scale bar = 200 μm

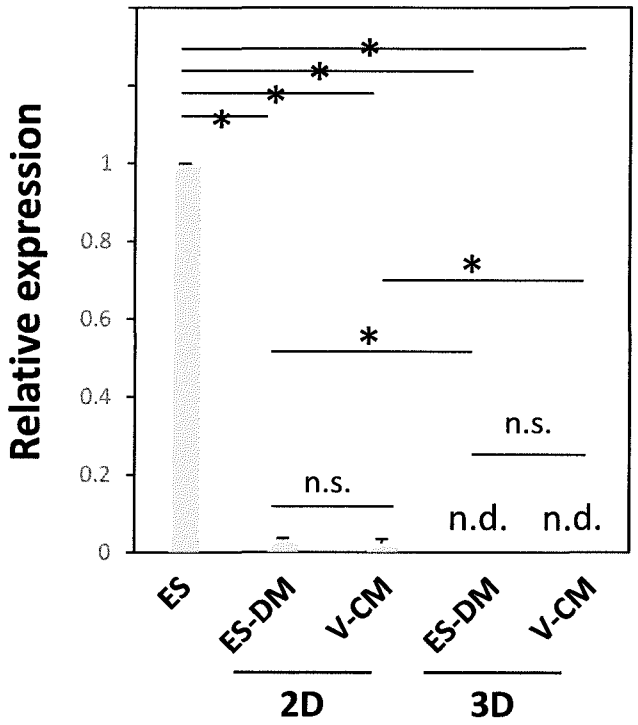

Fig. S5. Gene expression analysis of *Oct-3/4*, undifferentiated marker, in *Math1-GFP* ES cells under various conditions.

Gene expression of *Oct-3/4 in Math1-GFP* ES cells with or without cultivation using ES-DM or V-CM under 2D or 3D conditions was examined using real-time RT-PCR. Data were normalized to *β-actin* expression, used as an endogenous control. N=3, *$p < 0.05$, n.s.; not significant, n.d.; not detected

Table S1. Gene-specific primers used for real-time RT-PCR analysis

Genes	Primer sequences	Product size (bp)	GeneBank accession no.
Math1	Forward: 5'- AAATGTCGTATCTCTGCCTCTGGTC Reverse: 5'- AAGTACCCAATGCGGGTCTCAA	144	NM_007500.4
Myosin6	Forward: 5'- ATGGGCTGTGGGAACAGTGATA Reverse: 5'- CCCAAGAGTGTTGGTTGTCGAG	134	NM_001039546.2
Brn3c	Forward: 5'- ATGCGCCGAGTTTGTCTCC Reverse: 5'- AGGCTCTCATCAAAGCTTCCAAATA	68	NM_138945.2
Lmod3	Forward: 5'- TGAATGACATCCGACACAGCAA Reverse: 5'- GTTCGTGAAATGGCCTCCAG	123	NM_001081157.1
Dnah5	Forward: 5'- TGTTGTGTGCAATGAATGAGATGAC Reverse: 5'- TTGATGCCCACAATTCATTAGGAG	163	NM_133365.3
Oct-3/4	Forward: 5'- CAGACCACCATCTGTCGCTTC Reverse: 5'- AGACTCCACCTCACACGGTTCTC	194	NM_013633.3
β-actin	Forward: 5'-CATCCGTAAAGACCTCTATGCCAAC Reverse: 5'-ATGGAGCCACCGATCCACA	171	NM_007393.5

Table S2. Pathways enriched in DEGs

Direction	Adj. Pval	No. of genes	Pathway
Up-regulated	4.37E-17	44	Extracellular matrix organization
	4.37E-17	44	Extracellular structure organization
	4.37E-17	44	External encapsulating structure organization
	4.96E-17	154	Anatomical structure morphogenesis
	8.13E-16	96	Cell adhesion
	9.22E-16	216	System development
	1.01E-15	96	Biological adhesion
	4.65E-13	77	Animal organ morphogenesis
	1.72E-11	130	Nervous system development
	2.96E-09	103	Tissue development
	3.64E-09	155	Animal organ development
	9.46E-09	89	System process
	1.72E-08	43	Skeletal system development
	6.26E-08	96	Neurogenesis
	6.26E-08	110	Cell development
Down-regulated	8.73E-08	95	Cell adhesion
	8.73E-08	96	Biological adhesion
	2.74E-07	120	Tissue development
	2.01E-06	63	Cell-cell adhesion
	8.59E-06	150	Anatomical structure morphogenesis
	8.63E-06	32	Negative regulation of cell adhesion
	8.63E-06	79	Epithelium development
	1.17E-05	53	Tissue morphogenesis
	4.72E-05	46	Morphogenesis of an epithelium
	4.72E-05	24	Cell-cell junction organization
	4.78E-05	48	Transmembrane receptor protein tyrosine kinase signaling pathway
	4.91E-05	59	Actin filament-based process
	5.37E-05	173	Animal organ development
	6.73E-05	39	Epithelial cell proliferation
	7.99E-05	50	Negative regulation of cell differentiation

Table S3. List of genes with extracellular matrix organization enriched in DEGs

Egfl6, Loxl3, Ramp2, Tnr, Adamtsl4, Ntn4, Gfap, Fbln5, Col14a1, Col2a1, Vit, Adamts10, Kazald1, Col5a2, Col3a1, Postn, Col11a1, Sfrp2, Mmp16, Col15a1, Mmp23, Emilin1, Dmp1, Col1a2, Eln, Mmp2, Smpd3, Antxr1, Abi3bp, Ntng2, Adamtsl2, Ltbp4, Npnt, Fmod, Mfap4, Olfml2a, Foxc2, Lamb2, Adamts18, Col8a2, Adamts14, Col8a1, Serpinh1, Adamtsl3